Icarus 215 (2011) 603–607

Contents lists available at SciVerse ScienceDirect

Icarus

journal homepage: www.elsevier.com/locate/icarus

# Redefinition of the crater-density and absolute-age boundaries for the chronostratigraphic system of Mars

S.C. Werner [a,*], K.L. Tanaka [b]

[a] Physics of Geological Processes, University of Oslo, Sem Selands vei 24, NO-0316 Oslo, Norway
[b] Astrogeology Science Center, US Geological Survey, 2255N. Gemini Drive, Flagstaff, AZ 86001, USA

ARTICLE INFO

*Article history:*
Received 14 July 2010
Revised 22 July 2011
Accepted 22 July 2011
Available online 3 August 2011

*Keywords:*
Mars
Mars, Surface
Moon
Cratering
Geological processes

ABSTRACT

For the boundaries of each chronostratigraphic epoch on Mars, we present systematically derived crater-size frequencies based on crater counts of geologic referent surfaces and three proposed "standard" crater size–frequency production distributions as defined by (a) a simple −2 power law, (b) Neukum and Ivanov, (c) Hartmann. In turn, these crater count values are converted to model-absolute ages based on the inferred cratering rate histories. We present a new boundary definition for the Late Hesperian–Early Amazonian transition. Our fitting of crater size–frequency distributions to the chronostratigraphic record of Mars permits the assignment of cumulative counts of craters down to 100 m, 1 km, 2 km, 5 km, and 16 km diameters to martian epochs. Due to differences in the "standard" crater size–frequency production distributions, a generalized crater-density-based definition to the chronostratigraphic system cannot be provided. For the diameter range used for the boundary definitions, the resulting model absolute age fits vary within 1.5% for a given set of production function and chronology model ages. Crater distributions translated to absolute ages utilizing different curve descriptions can result in absolute age differences exceeding 10%.



## 1. Introduction

Formal detailed planet-wide stratigraphic systems have been derived for most terrestrial planets and satellites (e.g., Tanaka and Hartmann, in press). They are based on regional and global geologic mapping, and establish relative ages for surfaces and of units discriminated by superposition, morphology, albedo, composition, impact crater densities, and other features and relations (Wilhelms, 1990; Tanaka et al., 1994; Hansen, 2000). Mapping and stratigraphic analysis of Mars' global geologic structure was largely based on Viking Orbiter image data (Tanaka, 1986; Scott and Tanaka, 1986; Greeley and Guest, 1987; Tanaka and Scott, 1987) and is divided into three periods (Noachian, Hesperian, Amazonian), which have in total eight epoch subdivisions. Each of them was related to referent map units and crater densities (Tanaka, 1986; Tanaka et al., 1992). After Mars Global Surveyor (MGS; Orbital insertion date, 11 September 1997, Launch date, 7 November 1996), however, a clearer understanding of the physiographic characteristics and geologic evolution was afforded by topographic data of the Mars Orbital Laser Altimeter (MOLA) and additional image data of the Mars Orbiter Camera (MOC), both onboard MGS. In particular, Tanaka et al. (2003, 2005) used these datasets to significantly revise the discrimination and age of geological units in the northern plains (to be extended to a global map). Moreover, the updated map of the northern plains (Tanaka et al., 2005) resulted in two new definitions applied to the global stratigraphic scheme of Tanaka (1986). First, the pre-Noachian period was defined as the age of primordial crustal rocks underlying and predating but incorporated as fragments within Early Noachian outcrops. The second major change was to redefine the Early Amazonian referent as the Vastitas Borealis marginal and interior units.

The time-stratigraphic classification of the Vastitas Borealis units of Tanaka et al. (2005) is based mainly on superposition relations among the geologic units as well as the overall density of craters larger than 5 km in diameter for each unit from the crater catalog published by Barlow (1988, revised 2001) and the epoch boundary crater density values given by Tanaka (1986). Werner et al. (2011) revisited this time-stratigraphic evaluation by investigating the crater size–frequency distribution at selected type localities. That work revealed (1) possible resurfacing events recorded for craters <3 km in diameter, as well as (2) the lack of precise fits of crater size–frequency distributions to the Hesperian–Amazonian stratigraphic boundary as originally defined at multiple crater diameters. Nevertheless, that work showed that for craters >3 km in diameter, the statistical fit ages for the Vastitas Borealis units are quite uniform.

* Corresponding author.
*E-mail address:* stephanie.werner@fys.uio.no (S.C. Werner).

0019-1035/$ - see front matter © 2011 Elsevier Inc. All rights reserved.
doi:10.1016/j.icarus.2011.07.024

It also resulted in a revision of the 1 km reference crater frequency for the Hesperian–Amazonian boundary definition.

## 2. Brief summary of the crater counting technique

For optimal dating of cratered planetary surfaces, geologic mapping and crater count statistics need to be combined. Mapping provides delineation of materials by geomorphic and perhaps other characteristics based on natural breaks in the rock sequence, and crater count statistics provide a quantitative tool for defining relative ages and modeling absolute ages. The theoretical concept and mathematical background of age-dating techniques based on crater counts was developed in the 1960s and 1970s and summarized by the Crater Analysis Techniques Working Group (1979). The determination of model absolute ages on Mars and other solid surface objects is based on the application of a crater-production function and a cratering chronology model. The crater-production function describes the expected crater size–frequency distribution recorded in a geological unit at a specific time, and is, when scaled, comparable between planetary bodies such as the Moon and Mars (e.g., Neukum and Wise, 1976; Hartmann, 1977; Neukum and Ivanov, 1994; Ivanov, 2001). For the transfer from Moon to Mars one requires the flux ratio of impactors of various sizes between the lunar case to Mars considering celestial mechanical aspects and knowledge of how the conditions of crater formation differ from one planet to another. These conditions are mainly defined by the respective gravity and target properties of the impacted bodies and are accounted for by using appropriate crater scaling laws (e.g., Ivanov, 2001). The transfer of relative into absolute ages by the use of a chronology model is based on the assumptions that (1) the crater-production function – the original size–frequency distribution – is accurately known (e.g., Ivanov, 2001, originally in Neukum et al. (1975)) and stable with time, (2) the flux of projectiles onto the surfaces is isotropic, and (3) any target–property variations across the target body are negligible. With these assumptions, the crater densities measured on planetary surfaces that have been exposed for the same amount of time are equivalent in age. Relative ages based on the number of craters $N(D, t)$ are given for a fixed diameter $D$ (e. g., 1, 2, 4, 5, 10, 16 or 20 km); these are commonly referred to as "crater-retention ages" (Hartmann, 1966).

The crater chronology model applied is based on measurements of the crater size–frequency distribution on areas of the Moon, which are linked to radiometric ages retrieved from lunar rocks sampled and returned during the Apollo missions. This crater chronology model is transferable to other planets and solid surface bodies, assuming that all bodies have suffered from the same bombardment history (e.g., Hartmann, 1973; Soderblom et al., 1974; Neukum and Wise, 1976; Hartmann, 1978; Hartmann et al., 1981; Neukum and Hiller, 1981; Strom et al., 1992, and an attempt to unify in Hartmann and Neukum (2001)).

However, each standard crater size–frequency distribution is correlated with its individual lunar chronology model. Therefore, the diversity of crater size–frequency distribution (SFD) shapes (most recently e.g., Ivanov, 2001; Hartmann, 2005) and the combination of fitting the crater SFD and translation to absolute ages has resulted in differing definitions of the epoch boundaries (Hartmann and Neukum, 2001). Therefore, later attempts try to overcome this issue (e.g., Hartmann, 2005; Fassett and Head, 2008). While Hartmann (2005) suggested ranges in ages for each of the epoch boundaries, Fassett and Head (2008) used single representative boundary crater-density values as defined by Tanaka (1986) to anchor different production functions and to calculate the boundary definitions.

We offer a method that results in model ages and isochrons yet continues to reflect the major time-stratigraphic divisions that apply to the geologic history of Mars. We provide an approach to redefining the crater-density definitions for the martian epoch boundaries first described by Tanaka (1986) and updated for the Late Hesperian–Early Amazonian transition (Werner et al., 2011).

## 3. Crater-size frequency description

Traditionally there are two types of crater size–frequency distributions that are commonly used to portray crater densities on Mars: cumulative and incremental (which are binned) To enable comparison between these types, we sum the incremental version (Hartmann, 2005) and use it in a similar manner as other polynomial expressions, so that it is easy to calculate fitting parameters. According to the given incremental isochrons (Hartmann, 2005) we derived its individual cumulative production function. We compare these shapes with a minus-two power-law distribution (Fig. 1A) on which Tanaka (1986) fitted his counts for Hesperian and Amazonian lava flow units primarily for the 1–5 km diameter range. Comparing the three distribution descriptions using a two-sample Kolmogorov–Smirnov test limited to crater diameters between 1 km and 200 km, the two crater size–frequency distributions are similar to a simple −2 power-law distribution with a 91.6% confidence level. However, the two crater size–frequency distributions compared with each other reach only a confidence level of 87.5%. A similar comparison is shown by Ivanov (2001), who chose the incremental version for graphical display. In both descriptions, the differences between the two curve shapes are largest in the diameter range between 2 and 20 km with a maximum at about 7 km. The cumulative description used here is given in a polynomial form:

$$\log_{10} N_{cum} = \sum_{n=0}^{11} a_n [\log_{10}(D)]^n \quad (1)$$

with the coefficients $a_n$ listed in Table 1. $a_0$ is the parameter, which is used to shift the curve along the $y$-axis by a non-linear least-squares fit (Marquardt, 1963; Levenberg, 1944) and translates the crater frequencies to absolute ages. Commonly used martian chronology functions are: (1) $N\ (D \geqslant 1\ \text{km}) = 2.68 \times 10^{-14}\ (e^{6.93T}) - 1) + 4.13 \times 10^{-4}\,T$ (Ivanov, 2001), (2) $N\ (D \geqslant 1\ \text{km}) = 3.22 \times 10^{-14}\ (e^{6.93T}) - 1) + 4.875 \times 10^{-4}\,T$ (Hartmann and Neukum, 2001, presented only graphically) and (3) $N\ (D \geqslant 1\ \text{km}) = 4.4246 \times 10^{-14}\ (e^{6.93T}) - 1) + 6.8158 \times 10^{-4}\,T$ (derived from Hartmann (2005)), which result in progressively younger ages if fitted to the same measurement. The lunar chronology model is described by: $N\ (D \geqslant 1\ \text{km}) = 5.44 \times 10^{-14}\ (e^{6.93T}) - 1) + 8.38 \times 10^{-4}\,T$ (Neukum et al., 2001).

## 4. Revised chronostratigraphy for Mars

Global correlations of martian stratigraphy are based on mapped referents and crater densities (e.g., Tanaka, 1986; Tanaka et al., 2005). In areas where smaller-crater diameters were not counted previously, a simple extrapolation based on a minus-two sloped cumulative distribution was made for calculating reference crater densities (Tanaka, 1986). Model absolute ages can then be placed on these boundaries, based on fits of crater production curves (e.g., Hartmann and Neukum, 2001; Hartmann, 2005). However, these fits are not necessarily representative, because they depend on the choice of the crater production curves, which must fit crater-retention ages defined at multiple diameters. This makes it difficult to compare epoch assignments based on different combinations of chronology and production function. These variations are shown in Fig. 1. Tanaka (1986) used a range of diameters to define martian epoch boundaries based on a variety of published data as well as his own measurements. Moreover, progressively larger

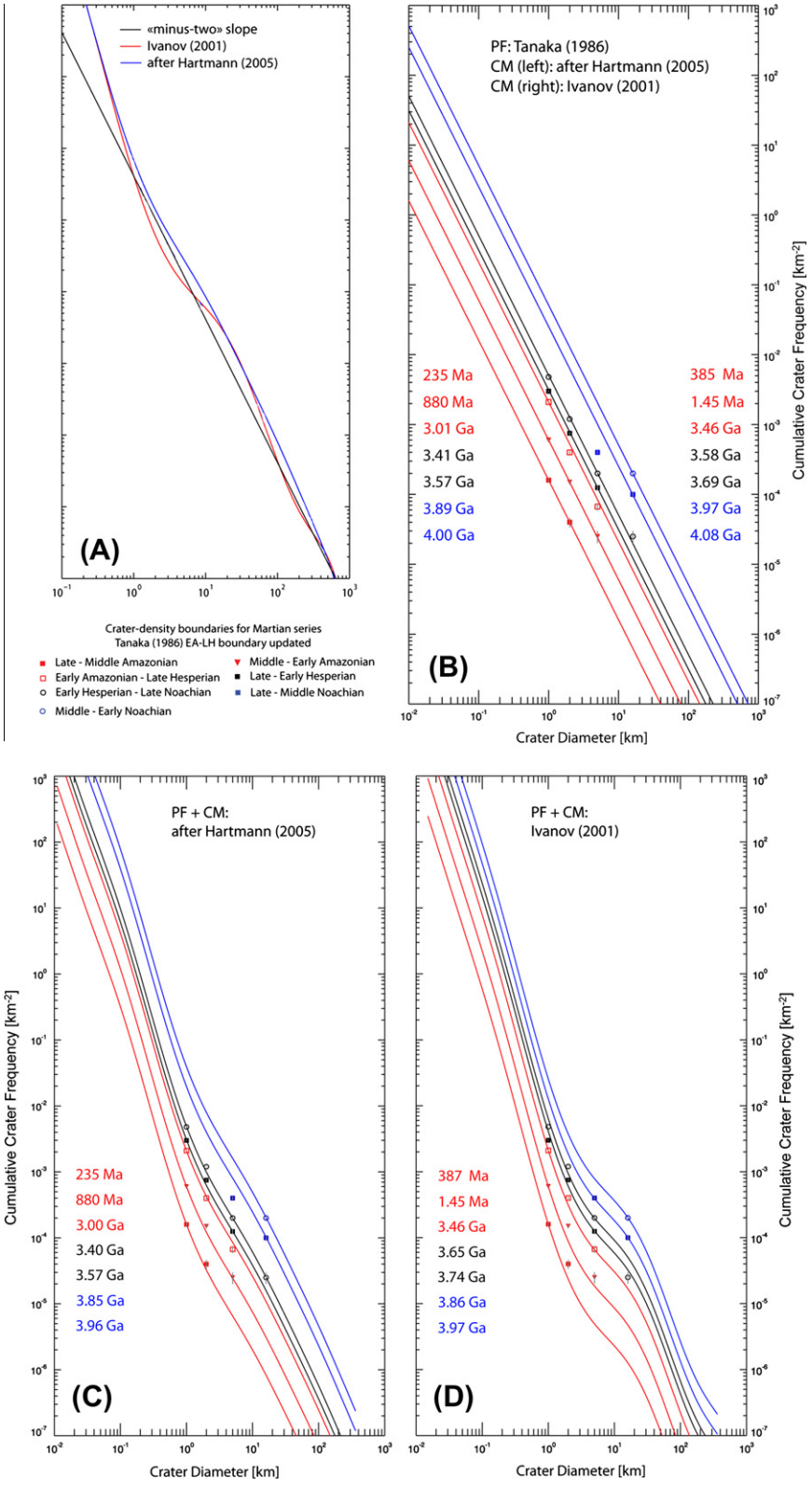


**Fig. 1.** Fits of the different crater size–frequency distributions to the boundary defining crater numbers according to Tanaka (1986) and Werner et al. (2011). The different cumulative crater size–frequency distributions are shown in comparison (A). Fits for the different polynomial production functions (PF) are given in (B) for a minus-two power law (following Tanaka, 1986), in (C) for a cumulative version of the incremental description by Hartmann (2005) following his 2004 version, and in (D) by Ivanov (2001). The polynomial coefficients are listed in Table 1. The resulting crater frequencies for diameters not described by Tanaka (1986) are given in Table 2. Absolute ages calculated using the chronology model (CM) of Ivanov (2001) are always older compared to that of Hartmann (2005) when calculated for the same fitted crater frequency.

diameters were useful to delineate older surfaces, due to their greater preservation vs. smaller craters. Now that crater production functions are commonly used to fit model ages to crater distributions, it is desirable that crater density boundaries for epochs should be fixed to particular diameters. From this baseline, one can fit a crater production function to the designated boundary

**Table 1**
Coefficients for the polynomial cumulative description according to Eq. (1).

| $n$ | Coefficients for the 11th order polynomial cumulative description | | |
|---|---|---|---|
| 11 | −0.00070349 | 0.00005805492 | 0 |
| 10 | 0.0023664 | 0.0006232845 | 0 |
| 9 | 0.0108278 | −0.004753462 | 0 |
| 8 | −0.04034 | −0.01180639 | 0 |
| 7 | −0.0568509 | 0.06755923 | 0 |
| 6 | 0.256181 | 0.1015683 | 0 |
| 5 | 0.109792 | −0.3630098 | 0 |
| 4 | −0.7735 | −0.4860814 | 0 |
| 3 | −0.0111926 | 0.7915374 | 0 |
| 2 | 1.25281 | 1.256814 | 0 |
| 1 | −2.65407 | −3.197453 | −2 |
| 0 | −3.1665[a] | −3.383677[a] | −3.383677[b] |
| | Derived from Hartmann (2005) | Ivanov (2001) | "Minus-two" |

[a] $a_0$ equivalent to a surface age of 1 Ga.
[b] $a_0$ equivalent to a surface age of 1 Ga following Ivanov (2001) and would be different following other chronology models.

and then define the boundary with a model absolute age. This then enables defining the model absolute age range for a given epoch based on the particular crater production function and the lunar vs. martian cratering ratio used.

For the Amazonian, we used the $N$ ($D \geqslant 1$ km) crater retention age values to define the epoch boundaries, as originally defined by Tanaka (1986) for the beginning of the Late and Middle Amazonian Epochs. However, given that Tanaka et al. (2005) redefined the beginning of the Early Amazonian as based on the Vastitas Borealis units, the new $N$ ($D \geqslant 1$ km) is assigned to $2100 \times 10^{-6}$ km$^{-2}$ based on recent counts by Werner et al. (2011). This value results from measurements in a few unit areas where no apparent resurfacing occurred; however, most of the units' surfaces have been modified to the extent that most craters smaller than 3 km in diameter seem to be obscured. In these cases, this number represents the extrapolated value of $N$ ($D \geqslant 1$ km) when the crater production function is fitted to the larger, more reliable crater diameter range ($D > 3$ km).

The beginning of the Late and Early Hesperian Epochs are defined by fits to $N$ ($D \geqslant 5$ km) of 125 and $200 \times 10^{-6}$ km$^{-2}$ respectively as defined in Tanaka (1986). Similarly, the beginning of the Late and Middle Noachian Epochs are based on the $N$ ($D \geqslant 16$ km) values of 100 and $200 \times 10^{-6}$ km$^{-2}$, respectively. We use a non-linear least-squares fit by preferentially weighting the above listed boundary values (and also printed in bold in Table 2). The weights are related to the size of the error bars, and our anchor points are considered to have no error, while the others have the uncertainties of the range listed by Tanaka (1986). Intercepts with $N$ ($D \geqslant 1$, 2, 5, and 16 km) can be calculated using the crater production function of Ivanov (2001), the cumulative version derived from Hartmann (2005), or a minus-two sloped distribution, and a martian to lunar cratering rate as discussed by Ivanov (2001) or a chronology function derived here which fits the Hartmann isochrons (Hartmann, 2005). The values are documented in Table 2. These new fits permit comparison of previously determined crater retention ages in the literature with this revised chronostratigraphy.

A statistical evaluation of the fit quality per epoch boundary is not significant due to the small number of points (between 1 and 4). On average, all the distributions represent the boundary definition within 99% confidence levels. The resulting age variations amount to 1–1.5% (Table 2) based on comparison of the given sets of production function and chronology model ages. However, if the best-fit relative age and the chronology function are not a homogeneous set, the errors can reach ~10%. For cratering statistics at smaller diameter ranges (less than 1 km), the crater size–frequency

**Table 2**
Crater frequencies and their model absolute ages for lower boundaries of martian epochs at specific crater diameters. For the fits different size–frequency distribution (SFD) shapes were used: (a) a minus-two-slope power law, (b) the description by Ivanov (2001), and (c) a cumulative version of the description by Hartmann (2005). The age is derived from the chronology model of (b) Ivanov (2001), and (c) derived from Hartmann (2005). The anchor points are printed in bold. The Early Noachian–Pre Noachian boundary defining crater density is an open issue.

| Epoch | $D \geqslant 100$ m per $10^6$ km$^2$ | | | $D \geqslant 1$ km per $10^6$ km$^2$ | | | $D \geqslant 2$ km per $10^6$ km$^2$ | | | $D \geqslant 5$ km per $10^6$ km$^2$ | | | $D \geqslant 16$ km per $10^6$ km$^2$ | | | Age (Ga) | | |
|---|---|---|---|---|---|---|---|---|---|---|---|---|---|---|---|---|---|---|
| | a | b | c | a | b | c | a | b | c | a | b | c | a | b | c | b | c |
| Late Amazonian | 16,000 | 590,608 | 319,032 | **160** | **160** | **160** | 40 | 24 | 33 | 6 | 5 | 7 | 1 | 1 | 1 | 0.387 | 0.235 |
| Middle Amazonian | 60,000 | 2.21478e+6 | 1.19637e+6 | **600** | **600** | **600** | 150 | 88 | 122 | 24 | 19 | 24 | 2 | 5 | 3 | 1.45 | 0.880 |
| Early Amazonian | 210,000 | 7.75173e+6 | 4.1873e+6 | **2100** | **2100** | **2100** | 525 | 309 | 427 | 84 | 65 | 86 | 8 | 17 | 11 | 3.46 | 3.00 |
| Late Hesperian | 312,500 | 1.4951e+7 | 6.11465e+6 | 3125 | 4050 | 3067 | 781 | 597 | 624 | **125** | **125** | **125** | 12 | 32 | 16 | 3.65 | 3.40 |
| Early Hesperian | 500,000 | 2.39216e+7 | 9.78344e+6 | 5000 | 6481 | 4907 | 1250 | 955 | 998 | **200** | **200** | **200** | 20 | 51 | 25 | 3.74 | 3.57 |
| Late Noachian | 2.56e+6 | 4.67571e+7 | 3.85129e+7 | 25,600 | 12,667 | 19,315 | 6400 | 1866 | 3930 | 1024 | 391 | 787 | **100** | **100** | **100** | 3.86 | 3.85 |
| Middle Noachian | 5.12e+6 | 9.35142e+7 | 7.70257e+7 | 51,200 | 25,334 | 38,630 | 12,800 | 3733 | 7859 | 2048 | 782 | 1575 | **200** | **200** | **200** | 3.97 | 3.96 |
| Early Noachian | | | | | | | | | | | | | | | | | |
| Pre-Noachian | | | | | | | | | | | | | | | | | |

[a] Derived according to fit a minus-two-slope power law (Fig. 1B), and values from Tanaka (1986), Tanaka et al. (2005) and Werner et al. (2011); those in bold are retained in our new scheme.
[b] Derived according to fit of Ivanov (2001) SFD in Fig. 1D.
[c] derived according to fit a cumulative version of Hartmann (2005) SFD in Fig. 1C.

distributions are incompatible with a simple −2 power-law distribution.

## 5. Open issues

The assignment of crater-density values to epoch boundaries for Mars relies on the caliber of the referents used and their ability to retain impact craters. It may be that future geologic mapping will establish improved referents for the epochs. Given that most surfaces on Mars have been exposed for billions of years and have been subjected to various resurfacing processes indicates that some inaccuracy is involved in the assignment of crater-density boundaries to the chronologic epochs. One open issue is whether the changing measured shape of the crater size–frequency distribution can be solely attributed to resurfacing processes or rather is due to a change in the projectile population (Barlow, 1990; Strom et al., 2005; Head et al., 2010). Additionally, as already pointed out by Ivanov (2001), Hartmann and Neukum (2001), as well as Fassett and Head (2008), the three crater production functions used here differ most in the diameter range between 2 and 20 km, and this requires a detailed description of the utilized function sets and boundary fits.

The crater chronology models applied here are based on measurements of the crater size–frequency distribution on areas of the Moon, which are linked to radiometric ages retrieved from lunar rocks sampled and returned during the Apollo missions. How the impactor flux evolves with time, which allows absolute ages to be derived from crater frequencies, is an area of active debate. It is uncertain whether the flux underwent a smooth decay or had one or more early peaks. Recent planetary formation models (Gomes et al., 2005; Tsiganis et al., 2005; Morbidelli et al., 2005) suggest that due to the migration of the giant gaseous planets within a disk of planetesimals, a cataclysmic Late Heavy Bombardment period of the terrestrial planets occurred. This potential Late Heavy Bombardment period would have occurred about 700 myr after the planets formed (3.9 Ga ago), based on the radiometric-dating of lunar rocks and their constituents thought to have formed during that period (e.g., Tera et al., 1974). Boundaries defined with absolute ages prior to 3.9 Ga will have to be assigned to different cratering rates. The precise shape of the cratering flux between 3.9 and 3.5 Ga is undergoing research (e.g., Morbidelli, 2010; Bottke et al., 2011). Moreover, occasional spikes in crater rate at Mars likely result from Main Belt asteroid family formation (Bottke et al., 2007).

## Acknowledgments

This paper benefited greatly from thorough reviews by Caleb Fassett and an anonymous reviewer. We appreciated comments by Michael Carr and Laurence Soderblom during internal USGS reviews. S.C.W. is supported by the Norwegian Research Council through a Centre of Excellence grant to PGP. K.L.T. is funded by a grant from the NASA Planetary Geology and Geophysics Program.

## References

Barlow, N.G., 1988. Crater size–frequency distributions and a revised martian relative chronology. Icarus 75, 285–305.
Barlow, N.G., 1990. Constraints on early events in martian history as derived from the cratering record. J. Geophys. Res. 95, 14191–14201.
Barlow, N. G. 2001. Status of the "Catalog of Large Martian Impact Craters" revision. American Astronomical Society, DPS Meeting 33, 36.13. Bull. Am. Astron. Soc. 33, 1105.
Bottke, W.F., Vokrouhlicky, D., Nesvorny, D., 2007. An asteroid breakup 160 Myr ago as the probable source of the K/T impactor. Nature 449, 48–53.
Bottke, W.F., et al., 2011. The great Archean bombardment, or the late late heavy bombardment. 42nd Lunar Planet. Sci. Abstract 2591.
Crater Analysis Techniques Working Group, Arvidson, R.E., Boyce, J., Chapman, C., Cintala, M., Fulchignoni, M., Moore, H., Neukum, G., Schultz, P., Soderblom, L., Strom, R., Woronow, A., Young, R., 1979. Standard and analysis of crater size–frequency data. Icarus 27, 464–474.
Fassett, C.I., Head III, J.W., 2008. The timing of martian valley network activity: Constraints from buffered crater counting. Icarus 195 (1), 61–89.
Greeley, R., Guest, J.E., 1987. Geological Map of the Eastern Equatorial Region of Mars (1:15,000,000), USGS.
Gomes, R., Levison, H.F., Tsiganis, K., Morbidelli, A., 2005. Origin of the cataclysmic Late Heavy Bombardment period of the terrestrial planets. Nature 435, 466–469.
Hansen, V.L., 2000. Geologic mapping of tectonic planets. Earth Planet. Sci. Lett. 176, 527–542.
Hartmann, W.K., 1966. Early lunar cratering. Icarus 5, 406–418.
Hartmann, W.K., 1973. Martian cratering 4: Mariner 9 initial analysis of cratering chronology. J. Geophys. Res. 78, 4096–4116.
Hartmann, W.K., 1977. Relative crater production rates on planets. Icarus 31, 260–276.
Hartmann, W.K., 1978. Martian cratering V: Toward an empirical martian chronology. Geophys. Res. Lett 5, 450–452.
Hartmann, W.K. et al., 1981. Chronology of planetary volcanism by comparative studies of planetary cratering. In: Basaltic Volcanism on the Terrestrial Planets. Pergamon Press, New York, pp. 1049–1128.
Hartmann, W.K., 2005. Martian cratering 8: Isochron refinement and the chronology of Mars. Icarus 174 (2), 294–320.
Hartmann, W.K., Neukum, G., 2001. Cratering chronology and the evolution of Mars. Space Sci. Rev. 96, 165–194.
Head, J.W. et al., 2010. Global distribution of large lunar craters: Implications for resurfacing and impactor populations. Science 329, 1504–1507.
Ivanov, B.A., 2001. Mars/Moon cratering rate ratio estimates. Space Sci. Rev. 96, 87–104.
Levenberg, K., 1944. A method for the solution of certain problems in least squares. Q. Appl. Math. 2, 164–168.
Marquardt, D., 1963. An algorithm for least-square estimation of nonlinear parameters. SIAM J. Appl. Math. 11, 431–441.
Morbidelli, A., Levison, H.F., Tsiganis, K., Gomes, R., 2005. Chaotic capture of Jupiter's Trojan asteroids in the early Solar System. Nature 435, 462–465.
Morbidelli, A., 2010. A coherent and comprehensive model of the evolution of the outer Solar System. C. R. Phys. 11, 651–659.
Neukum, G., Hiller, K., 1981. Martian ages. J. Geophys. Res. 86 (15), 3097–3121.
Neukum, G., Ivanov, B.A., 1994. Crater size distributions and impact probabilities on Earth from lunar, terrestrial-planet, and asteroid cratering data. In: Hazards Due to Comets and Asteroids, pp. 359–416.
Neukum, G., Wise, D.U., 1976. Mars – A standard crater curve and possible new time scale. Science 194, 1381–1387.
Neukum, G., König, B., Arkani-Hamed, J., 1975. A study of lunar impact crater size-distributions. Moon 12, 201–229.
Neukum, G., Ivanov, B.A., Hartmann, W.K., 2001. Cratering records in the inner solar system in relation to the lunar reference system. Space Sci. Rev. 96, 55–86.
Scott, D.H., Tanaka, K.L., 1986. Geological Map of the Western Equatorial Region of Mars (1:15,000,000), USGS.
Soderblom, L.A., Condit, C.D., West, R.A., Herman, B.M., Kreidler, T.J., 1974. Martian planetwide crater distributions – Implications for geologic history and surface processes. Icarus 22, 239–263.
Strom, R.G., Croft, S.K., Barlow, N.G., 1992. The martian impact cratering record. In: Mars, pp. 383–423.
Strom, R.G., Malhotra, R., Ito, T., Yoshida, F., Kring, D.A., 2005. The origin of planetary impactors in the inner Solar System. Science 309, 1847–1850.
Tanaka, K.L., 1986. The stratigraphy of Mars. J. Geophys. Res. 91, 139–158.
Tanaka, K.L., et al., 1994. The Venus Geologic Mappers' Handbook, US Geological Survey Open-File Report 94-438, 66 pp.
Tanaka, K.L., Scott, D.H., 1987. Geological Map of the Polar Regions of Mars (1:15,000,000), USGS.
Tanaka, K.L., Scott, D.H., Greeley, R., 1992. Global stratigraphy. In: Mars, pp. 345–382.
Tanaka, K.L., Skinner, J.A., Hare, T.M., Joyal, T., Wenker, A., 2003. Resurfacing history of the northern plains of Mars based on geologic mapping of Mars Global Surveyor data. J. Geophys. Res. 108, 24.
Tanaka, K.L., Skinner, J.A., Hare, T.M., 2005. Geological Map of the Northern Plains of Mars (1:15,000,000), USGS. <http://pubs.usgs.gov/sim/2005/2888/>.
Tanaka, K.L., Hartmann, W.K., in press. Planetary time scale. In: Gradstein, F.M., Ogg, J.G., Smith, A.G., (Eds.), A Geologic Time Scale 2012. Cambridge University Press.
Tera, F., Papanastassiou, D., Wasserburg, G., 1974. Isotopic evidence for a terminal lunar cataclysm. Earth Planet. Sci. Lett. 2, 1–21.
Tsiganis, K., Gomes, R., Morbidelli, A., Levison, H.F., 2005. Origin of the orbital architecture of the giant planets of the Solar System. Nature 435, 459–461.
Werner, S.C., Tanaka, K.L., Skinner Jr., J.A., 2011. Mars: The evolutionary history of the northern lowlands based on crater counting and geologic mapping. Planet. Space Sci. 59, 1143–1165.
Wilhelms, D.E., 1990. Geologic mapping. In: Greeley, R, Batson, R.M. (Eds.), Planetary Mapping. Cambridge University Press, New York, pp. 208–260.